Theor Chim Acta (1988) 74: 381-402

Theoretica Chimica Acta

A new method for the direct calculation of resonance parameters with application to the quasibound states of the $H_2X\ ^1\Sigma_g^+$ system

David W. Schwenke*
Eloret Institute, Palo Alto, CA 94303, USA

(Received November 24, 1987/Accepted March 2, 1988)

A new method for the direct calculation of resonance parameters is presented. It is based upon searching for poles of the scattering matrix at complex energies. This search is expedited by the use of analytic derivatives of the scattering matrix with respect to the total energy. This procedure is applied initially to a single channel problem, but is generalizable to more complicated systems. Using the most accurate available potential energy data, we calculate resonance parameters for all of the physically important quasibound states of the ground electronic state of the hydrogen molecule. Corrections to the Born-Oppenheimer potential are included and assessed. The new method has no difficulty locating resonances with widths greater than about 1×10^{-7} cm^{-1}. It is easier to find narrow resonances by monitoring the dependence of the imaginary part of the reactance matrix on the real part of a complex energy than to monitor the dependence of the eigenphase sum on energy at real energies.

Key words: Resonance — Complex energy — Derivatives

1. Introduction

Resonances take part in a wide variety of physical phenomena [1], thus a detailed understanding of resonant processes is an important theoretical goal. The particular physical process motivating the present study is the three body recombination of hydrogen atoms to form hydrogen molecules. A detailed theoretical

* *Mailing address*: NASA Ames Research Center, Moffett Field, CA 94035, USA

description of three body recombination kinetics requires as input the identity of the important quasibound states involved in the recombination process [2]. Part of the information necessary to discriminate between the important and unimportant resonances are the energies and lifetimes, which will be calculated here using a new computational method. Although in the present paper the new method is only applied to a single channel problem, the techniques developed here are more general.

Quasibound states, or resonances, are bound states at complex energies while true bound states occur at negative real energies [3]. At real energies near the resonance energy, the scattering states share many features with true bound states, the main exception being that they have nonzero decay life times.

A resonance is completely characterized by the location of the bound state energy in the complex energy plane as well as the residue of the scattering matrix at that energy. All of these quantities can be determined indirectly from calculations at real energies [4–7], however, calculations at only real energies do not produce unique results because of the fitting procedures involved. Part of the difficulty stems from the interference between resonant scattering and background scattering as well as the possibility of interference between overlapping resonances. Additional complications arise because different interpretations of the physical processes by which resonances are manifested can lead to different methods of calculating some of the resonance parameters [8]. One great advantage of calculations at complex energy is that none of these ambiguities arise. In spite of this advantage, there have been relatively few studies where all resonance parameters were obtained from scattering calculations at complex energies [9, 10].

For the hydrogen molecule, there have been several determinations of the resonance energies [11–14] (the real part of the complex bound state energy) and some of the resonance widths [12–13] (the negative of twice the imaginary part of the complex bound state energy), but none of the partial widths (the absolute value of the residue). These studies were restricted to calculations at real energies and the calculations of the resonance widths used potential energy data which has since been improved [15–16]. In this paper we directly calculate all of the resonance parameters for the important H_2 quasibound states using the most accurate available potential data, included corrections to the Born–Oppenheimer potential. Our results are compared to previous determinations of the resonance parameters as well as to some simpler methods and to experiment when possible. We will see that the current method is a very powerful way to determine the resonance parameters for resonances which vary from being quite broad to extremely narrow.

2. Theory

The Schrödinger equation describing the time independent collision of two particles can be written as

$$d^2 f_{nn_0}(r)/dr^2 = \sum_{n'} \{\delta_{nn'}[l_{n'}(l_{n'}+1)/r^2 - k_{n'}^2] + 2\mu\hbar^{-2} V_{nn'}(r)\} f_{n'n_0}(r), \tag{1}$$

where each n defines a channel, l_n is the orbital angular momentum for channel n, k_n is the wave vector for channel n given by

$$k_n^2 = 2\mu(E-\epsilon_n)/\hbar^2, \tag{2}$$

where μ is the reduced mass for the collision process, E is the total energy, ϵ_n is the eigenenergy of channel n, and $V_{nn'}$ is a potential matrix element. Eq. (1) is solved for the unknown radial functions $f_{nn'}$ which are subject to the boundary conditions

$$f_{nn'}(r) \sim 0 \quad \text{as } r \sim 0, \tag{3}$$

$$f_{nn'}(r) \sim \delta_{nn'} h_n^{(2)}(r) + h_n^{(1)}(r) S_{nn'} \quad \text{as } r \sim \infty, \tag{4}$$

where $S_{nn'}$ is a scattering matrix element and the matching functions are given by

$$h_n^{(1)}(r) = k_n^{1/2}[j_{l_n}(k_n r) + i y_{l_n}(k_n r)] \tag{5}$$

and

$$h_n^{(2)}(r) = k_n^{1/2}[j_{l_n}(k_n r) - i y_{l_n}(k_n r)], \tag{6}$$

j_l and y_l being the Riccati-Bessel functions which go asymptotically as sin and $-\cos$. From the scattering matrix, the physical observables for the scattering process can be calculated.

We will define a resonance to be manifested by a pole in the scattering matrix in the complex energy plane with Re $E > 0$ and Im $E < 0$ [3]. At these energies, the scattering wavefunction is essentially square integrable since the wavefunction will only contain exponentially decreasing components $[h^{(1)}(k_n r) \propto \exp(-\text{Im}[k_n r]) \exp\{i(\text{Re}[k_n r] - l_n \pi/2)\}$ as $r \sim \infty]$. It should be noted that if the matching functions $h^{(1)}$ and $h^{(2)}$ are interchanged in the boundary conditions specified by Eq. (4), the inverse of the scattering matrix appears in that equation instead of the scattering matrix. This is useful because where the scattering matrix has a pole, the inverse will have a zero, which is more convenient to handle numerically.

In general, in the vicinity of a resonance, the energy dependence of the scattering matrix will take the form [17]

$$S_{nn'} = S_{nn'}^b - \frac{i\gamma_{\alpha n}\gamma_{\alpha n'}}{z_\alpha - E}, \tag{7}$$

where $S_{nn'}^b$ is a background, nonresonant contribution which varies slowly with energy, α labels a particular resonance, $\gamma_{\alpha n}$ is a partial width amplitude, and z_α is the position of the pole in the complex energy plane. A useful diagnostic at real energies for the detection of the presence of a resonance is to consider the energy dependence of the eigenphase sum Δ defined by

$$\det \boldsymbol{S} = \exp(2i\Delta). \tag{8}$$

Normally for molecular systems, Δ decreases as the energy increases, but in the vicinity of a resonance, Δ suddenly increases by π as the energy is increased [18].

It is useful to define the observable quantities $\mathscr{E}_\alpha$, Γ_α and $\Gamma^0_{\alpha n}$ by

$$z_\alpha = \mathscr{E}_\alpha - i\Gamma_\alpha/2, \tag{9}$$

and

$$\Gamma^0_{\alpha n} = |\gamma_{\alpha n}|^2. \tag{10}$$

$\mathscr{E}_\alpha$ is called the resonance energy, Γ_α the total resonance width and $\Gamma^0_{\alpha n}$ a partial width. The resonance energy is the physically obtainable energy where the scattering due to the resonance is most important. The total resonance width controls both the energy range over which the resonance scattering is observed and also the decay rate of the resonant state. In particular, the resonant state decays with an unimolecular rate equal to $\Gamma_\alpha/\hbar$. In a multichannel problem, the partial widths control the branching ratios to the various final states when the resonant state decays.

It can be shown that in the vicinity of an isolated, narrow resonance (INR) [17], that the partial widths sum up to the total resonance width:

$$\Gamma_\alpha = \sum_n \Gamma^0_\alpha. \tag{11}$$

However, previous experience [7] indicates that when a resonance is not isolated and narrow, usually Eq. (11) becomes an inequality with the partial width being less than the total width. Some previous studies [4-6] which determined partial widths constrained them to satisfy Eq. (11). In the present study, we directly determine the resonance energy and total width from Eq. (9) after determining the energy z_α which gives rise to a pole in the scattering matrix. In addition, we determine the partial widths by numerically evaluating the contour integral

$$\oint S_{nn'}(E)\, dE = 2\pi\gamma_{\alpha n}\gamma_{\alpha n'}. \tag{12}$$

Thus using our procedure, it is not necessary to make any assumption about the background contribution $S^b_{nn'}$ or whether or not Eq. (11) is satisfied.

3. Numerical methods

This section will be broken up into five subsections. First we describe how we proceed with the search for the pole, which motivates our algorithm for solving Eq. (1). Then this algorithm is discussed, followed by methods for determining initial guesses for the pole energy. Next we consider some subtleties concerning large r behavior of the potential and finally we discuss how we extrapolate to the limit of zero stepsize.

Our initial application is to the collision of two hydrogen atoms. In this case, there is only one term in the sum of Eq. (1) and we take our zero of energy so that ϵ_1 is zero. Individual resonances will be labeled by $\alpha = (v, J)$, where v indicates the number of nodes in the wave function inside the potential maximum and J indicates the angular momentum of the system (i.e. $l_1 = J$). For our initial

tests, we use the potential of [11]—we denote this the WB potential—and we take the reduced mass μ to be 918.575728 a.u., since this appears to be close to the value used in [12]. All of our calculations are carried out using Hartree atomic units and the final energies are converted to cm^{-1} by division by the factor 4.556335×10^{-6}.

3.1. Searching for the pole

It is numerically inconvenient to search for the pole of the scattering matrix. Instead, we will search for the zero of the inverse of the scattering matrix.

One of the most powerful methods for determining a zero of a multidimensional function is the Newton-Raphson procedure [19]. In this procedure, applied to the present problem, given a guess to the energy of the zero at iteration j, z_j, the improved estimate for the zero is

$$z_{j+1} = z_j + \delta, \tag{13}$$

where δ is determined from the matrix relation

$$d = -\boldsymbol{J}^{-1} \boldsymbol{f}, \tag{14}$$

where

$$d_1 = \mathrm{Re}\ \delta, \tag{15}$$

$$d_2 = \mathrm{Im}\ \delta, \tag{16}$$

$$f_1 = \mathrm{Re}\ \det \boldsymbol{S}^{-1}(z_j), \tag{17}$$

$$f_2 = \mathrm{Im}\ \det \boldsymbol{S}^{-1}(z_j), \tag{18}$$

$$J_{11} = J_{22} = \mathrm{Re}\ d\ \det \boldsymbol{S}^{-1}/dz|_{z=z_j}, \tag{19}$$

$$J_{21} = -J_{12} = \mathrm{Im}\ d\ \det \boldsymbol{S}^{-1}/dz|_{z=z_j}, \tag{20}$$

where $\det \boldsymbol{S}^{-1}$ is the determinant of the inverse of the scattering matrix. For the present application, $\det \boldsymbol{S}^{-1}$ is simply S_{11}^{-1}. In the vicinity of the root, the Newton-Raphson procedure converges quadratically. We have found that this procedure converges quite well provided z_j is sufficiently close to the root energy. If z_j is not sufficiently close, $|\det \boldsymbol{S}^{-1}(z_{j+1})|$ will be further from zero than $|\det \boldsymbol{S}^{-1}(z_j)|$ was and we try scaling δ in Eq. (13) by multiples of 1/2 until an energy is produced which has $|\det \boldsymbol{S}^{-1}|$ closer to zero than $|\det \boldsymbol{S}^{-1}(z_j)|$ was. Sometimes, especially for narrow resonances, it is advantageous to enforce a limit on the maximum change in z to keep the estimates from wandering away from the zero. If z_j is too far from the root energy, then the search fails to find the root.

As mentioned in Sect. 2 we calculate the partial widths by evaluating Eq. (12). The particular contour we use is a square one with a side of length $\Gamma_\alpha/5$ centered on the pole. The integral along each side is evaluated using Gauss-Legendre quadrature with typically 6 points per side required to converge the results to about 0.1%.

If, as in the present application, only one channel is involved and $\det \boldsymbol{S}^{-1}$ is the same as $\boldsymbol{S}^{-1}$, the Newton-Raphson scheme is the most natural procedure. However, in multichannel applications, it might be more advantageous to search for an energy which zeros each $[\boldsymbol{S}^{-1}]_{nn'}$ individually — this gives rise to a nonlinear least squares procedure. Previous workers have considered both choices [9, 10].

An important reason for the fast convergence of the Newton-Raphson procedure is the presence of the derivative. The derivative of the scattering matrix with respect to energy is not usually a by-product of a scattering calculation, and requires a special algorithm to calculate it.

3.2. Calculating the derivative of the scattering matrix

The procedure we will use to calculate the scattering matrix and its derivative is a modification of the R matrix propagation algorithm [20]. In the equations below, bold face quantities will denote matrices. In the discussion that follows, the standard R matrix propagation algorithm is used to just calculate $\boldsymbol{R}_4$, while we modify it to also calculate $\partial \boldsymbol{R}_4/\partial E$.

Derivatives of the scattering matrix can be obtained from integrals of the wave function [21], however, this may be undesirable for two reasons. First of all, most numerical algorithms which are stable with respect to including closed channels (such as the R matrix propagation algorithm) do not directly yield the wave function, and it is not necessarily possible to extract an accurate wave function from them. Secondly some sort of numerical quadrature would usually be involved to evaluate the integral, and this can produce numerical error. The method proposed below is free of both of these problems.

We rewrite Eq. (1) in the form

$$d^2\boldsymbol{f}/dr^2 = \boldsymbol{D}(r)\boldsymbol{f}(r), \tag{21}$$

where

$$D_{nn'} = \{\delta_{nn'}[l_n(l_n+1)/r^2 - k_n^2] + 2\mu\hbar^{-2}V_{nn'}(r)\}. \tag{22}$$

We integrate Eq. (21) from $r = r_0$, where $\boldsymbol{f}$ is negligible, to $r = r_{asy}$, where the potential is negligible. The range r_0 to r_{asy} is divided up into M sectors with centers r_j and widths h_j such that $r_0 = r_1 - h_1/2$ and $r_{asy} = r_M + h_M/2$. In each sector we assume $\boldsymbol{D}$ is independent of r, and we take its value to be $\boldsymbol{D}(r_j)$ for sector j and call it $\boldsymbol{D}^{(j)}$. Thus we can uncouple Eq. (21) by applying the transformation $\boldsymbol{T}^{(j)}$ which diagonalizes $\boldsymbol{D}^{(j)}$. The uncoupled equations are then solved analytically using the Magnus propagator. To make the solution numerically stable, instead of directly determining the wavefunction $\boldsymbol{f}$, in this algorithm one determines the quantity $\boldsymbol{R}_4$ defined by

$$\boldsymbol{R}_4(r') = -\boldsymbol{f}(r')[d\boldsymbol{f}/dr|_{r=r'}]^{-1}. \tag{23}$$

Making the definition that $\boldsymbol{R}_4^{(j)}$ is $\boldsymbol{R}_4$ evaluated at $r_j + h_j/2$, then the R matrix

propagation equations can be written

$$\boldsymbol{R}_4^{(j)} = \boldsymbol{r}_4^{(j)} - \boldsymbol{r}_3^{(j)} \boldsymbol{M}(j-1,j) \boldsymbol{r}_2^{(j)}, \tag{24}$$

$$\boldsymbol{M}(j-1,j) = [\boldsymbol{R}_4^{(j-1)} + \boldsymbol{r}_1^{(j)}]^{-1}, \tag{25}$$

$$\boldsymbol{r}_1^{(j)} = \mathcal{T}(j-1,j) \boldsymbol{P}_1^{(j)} [\boldsymbol{P}_3^{(j)}]^{-1} [\mathcal{T}(j-1,j)]^{-1}, \tag{26}$$

$$\boldsymbol{r}_2^{(j)} = \mathcal{T}(j-1,j) [\boldsymbol{P}_3^{(j)}]^{-1}, \tag{27}$$

$$\boldsymbol{r}_3^{(j)} = [\boldsymbol{P}_3^{(j)}]^{-1} [\mathcal{T}(j-1,j)]^{-1}, \tag{28}$$

$$\boldsymbol{r}_4^{(j)} = [\boldsymbol{P}_3^{(j)}]^{-1} \boldsymbol{P}_1^{(j)}, \tag{29}$$

$$\mathcal{T}(j-1,j) = \boldsymbol{T}^{(j-1)T} \boldsymbol{T}^{(j)}, \tag{30}$$

$$[\boldsymbol{P}_1^{(j)}]_{nn'} = \delta_{nn'} \cos(-h_j \lambda_n^{(j)}), \tag{31}$$

$$[\boldsymbol{P}_3^{(j)}]_{nn'} = -\delta_{nn'} \lambda_n^{(j)} \sin(-h_j \lambda_n^{(j)}), \tag{32}$$

and

$$\sum_{n',n''} T_{n'n}^{(j)} D_{n'n''}^{(j)} T_{n''n_0}^{(j)} = \delta_{nn_0} \lambda_n^{(j)2}. \tag{33}$$

Equations (31) and (32) remain valid as $\lambda_n^{(j)}$ becomes complex. In the first sector, we have

$$\boldsymbol{R}_4^{(1)} = \boldsymbol{r}_4^{(1)}. \tag{34}$$

We now wish to calculate $\partial \boldsymbol{R}_4^{(j)}/\partial E$. To do this, differentiate Eq. (24):

$$\begin{aligned} \partial \boldsymbol{R}_4^{(j)}/\partial E = {} & \partial \boldsymbol{r}_4/\partial E - \partial \boldsymbol{r}_3^{(j)}/\partial E \boldsymbol{M}(j-1,j) \boldsymbol{r}_2^{(j)} \\ & + \boldsymbol{r}_3^{(j)} \boldsymbol{M}(j-1,j) [\partial \boldsymbol{R}_4^{(j-1)}/\partial E + \partial \boldsymbol{r}_1^{(j)}/\partial E] \boldsymbol{M}(j-1,j) \boldsymbol{r}_2^{(j)} \\ & - \boldsymbol{r}_3^{(j)} \boldsymbol{M}(j-1,j)\, \partial \boldsymbol{r}_2^{(j)}/\partial E. \end{aligned} \tag{35}$$

The derivatives on the right hand side of Eq. (35) are easily evaluated from Eqs. (24)-(29) to yield

$$\partial \boldsymbol{r}_1^{(j)}/\partial E = \mathcal{T}(j-1,j)\, \partial \boldsymbol{r}_4^{(j)}/\partial E [\mathcal{T}(j-1,j)]^{-1}, \tag{36}$$

$$\partial \boldsymbol{r}_2^{(j)}/\partial E = \mathcal{T}(j-1,j)\, \partial [\boldsymbol{P}_3^{(j)}]^{-1}/\partial E, \tag{37}$$

$$\partial \boldsymbol{r}_3^{(j)}/\partial E = \partial [\boldsymbol{P}_3^{(j)}]^{-1}/\partial E [\mathcal{T}(j-1,j)]^{-1}, \tag{38}$$

$$\partial \boldsymbol{r}_4^{(j)}/\partial E = \partial [\boldsymbol{P}_3^{(j)}]^{-1}/\partial E \boldsymbol{P}_1^{(j)} + [\boldsymbol{P}_3^{(j)}]^{-1}\, \partial \boldsymbol{P}_1^{(j)}/\partial E. \tag{39}$$

The final derivatives required are

$$\partial [\boldsymbol{P}_1^{(j)}]_{nn'}/\partial E = -\delta_{nn'} \mu h_j \sin(-h_j \lambda_n^{(j)})/\lambda_n^{(j)} \hbar^2, \tag{40}$$

and

$$\partial [\boldsymbol{P}_3^{(j)}]^{-1}/\partial E = -[\boldsymbol{P}_3^{(j)}]^{-2}\, \partial \boldsymbol{P}_3^{(j)}/\partial E, \tag{41}$$

$$\partial [\boldsymbol{P}_3^{(j)}]_{nn'}/\partial E = -\delta_{nn'} \mu [-\sin(-h_j \lambda_n^{(j)}) + h_j \lambda_n^{(j)} \cos(-h_j \lambda_n^{(j)})]/\lambda_n^{(j)} \hbar^2. \tag{42}$$

In deriving Eqs. (36)-(39) we have used the fact that when the potential is independent of energy, $\boldsymbol{D}^{(j)}$ can be written as the sum of an energy independent full matrix minus $2\mu E/\hbar^2$ times the unit matrix and so the $\boldsymbol{T}^{(j)}$ are independent of energy and

$$\partial\lambda_n^{(j)}/\partial E = -\mu/\lambda_n^{(j)}\hbar^2. \tag{43}$$

From $\boldsymbol{R}_4$ and $\partial\boldsymbol{R}_4/\partial E$ we can calculate the scattering matrix and its derivative. The result is

$$\boldsymbol{S} = -(\boldsymbol{h}^{(1)} + \boldsymbol{R}_4^{(M)}\, d\boldsymbol{h}^{(1)}/dr)^{-1}(\boldsymbol{h}^{(2)} + \boldsymbol{R}_4^{(M)}\, d\boldsymbol{h}^{(2)}/dr) \tag{44}$$

and

$$\begin{aligned}\partial\boldsymbol{S}/\partial E = -(\boldsymbol{h}^{(1)} + \boldsymbol{R}_4^{(M)}\,\partial\boldsymbol{h}^{(1)}/\partial r)^{-1}[&\partial\boldsymbol{R}_4^{(M)}/\partial E(\partial\boldsymbol{h}^{(2)}/\partial r + \partial\boldsymbol{h}^{(1)}/\partial r\boldsymbol{S}) \\ &+(\partial\boldsymbol{h}^{(2)}/\partial E + \partial\boldsymbol{h}^{(1)}/\partial E\boldsymbol{S}) + \boldsymbol{R}_4^{(M)}(\partial^2\boldsymbol{h}^{(2)}/\partial r\,\partial E + \partial^2\boldsymbol{h}^{(1)}/\partial r\,\partial E\boldsymbol{S})],\end{aligned} \tag{45}$$

where the matching functions and their derivatives are evaluated at r_{asy} and are diagonal with diagonal elements given by Eqs. (5)-(6), etc.

It should be noted that the R matrix propagation algorithm solves exactly the scattering problem in which the actual coupling matrix $\boldsymbol{D}(r)$ is replaced by the "stair step" coupling matrix $\boldsymbol{D}^{(j)}$. This means that Eq. (45) for the derivative of the scattering matrix is exact also. Just as the resonance parameters obtained are a function of the potential used, they will by a function of the integration stepsize used. This point is discussed further below in Sect. 3.5.

3.3. The determination of the initial guess for z_α

Our experience is that the Newton-Raphson procedure only converges if the initial guess for the pole position is reasonably close to the accurate value. In this case, close means that the guess for $\mathscr{E}_\alpha$ is within a few multiples of Γ_α to the accurate value and the guess for Γ_α is within about an order of magnitude of the accurate value. For this particular problem ($H_2X\,{}^1\Sigma_g^+$), we can use the previously determined resonance energies and widths as initial guesses, however, in some cases these are not good enough (not necessarily because they are not sufficiently accurate - see the discussion in Sect. 3.5.), and so we use more general procedures.

We initially determine estimates of the resonance parameters by performing a stabilization calculation at real energies. To do this calculation, we use the 11-point finite difference boundary value method [22] (FDBV) to determine the eigenvalues of the potential imbedded in a spherical box of variable radius. The resonance energy is identified as an energy where the ratio of the average wave function amplitude inside the centrifugal barrier maximum to the average wave function amplitude outside the barrier for a particular eigenvalue is maximized as a function of the size of the spherical box. This is similar to the procedure of [23]. The resonance widths are estimated from the variation of the resonant eigenvalue with the size of the box [24]. Sometimes when the widths are too small, this

method fails to give a good estimate of the width. In this case a semiclassical procedure is used [25]. Here the width is given by

$$\Gamma_\alpha = \hbar\omega \exp(-2I), \tag{46}$$

where ω is the classical vibrational period and I is the barrier penetration integral given by

$$I = \hbar^{-1} \int_{r_2}^{r_3} [2\mu(V-E)]^{1/2} dr, \tag{47}$$

where r_2 and r_3 are the turning points for the tunneling region. We evaluate the vibrational period by differentiating the classical action integral. All integrals over the potential are calculated using converged Gauss-Legendre quadrature.

If the resonance width is greater than about 0.1 cm^{-1}, the FDBV estimate provides a sufficiently accurate guess for the Newton-Raphson procedure to converge to the pole. If the width is smaller, it is necessary to obtain a more accurate estimate of the resonance energy. We obtain this as follows. On the real energy axis, the reactance matrix defined by

$$\boldsymbol{R} = i(\mathbf{1}+\boldsymbol{S})^{-1}(\mathbf{1}-\boldsymbol{S}) \tag{48}$$

is real while at the pole energy, it is purely imaginary. Thus it might be expected that the presence of the pole might manifest itself in a wider energy range in the complex energy plane than on the real energy axis. We then perform a series of calculations varying the resonance energy but keeping the resonance width fixed. In these calculations, we look only at the imaginary part of the reactance matrix, and seek an energy which makes Im (R_{11}) closest to $-i$. Once this improved estimate of the resonance energy is determined, we improve the estimate of the resonance width by roughly optimizing the resonance width at fixed resonance energy. This estimate of the resonance energy and width is then used as input to the Newton-Raphson procedure. We found that this procedure works quite well for most resonances and is not strongly dependent on the initial guess for the resonance width. The exception occurs for resonances with extremely small widths ($<10^{-7}$ cm^{-1}). The reason for the failure for extremely small widths is that for these widths, the finite number of digits available on the computer makes it impossible to represent the resonance energy to enough digits so that the difference between it and the accurate resonance energy is less than a few multiples of the resonance width (all of our calculations were performed on the AMES ACF Cray-X/MP 48 using 64 bit precision).

Figure 1 shows a plot of both Im (R_{11}) and the eigenphase sum as a function of energy for energies in the vicinity of the $J = 13$ resonance. There we see how the resonance is manifested over a much broader energy range in Im (R_{11}) than in the eigenphase sum, which is the usual function monitored when searching for resonance.

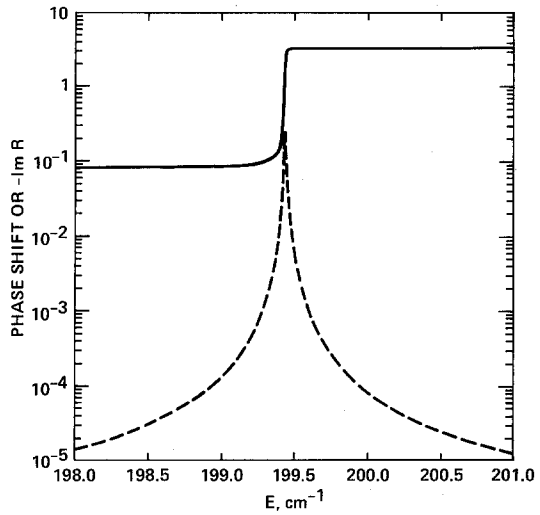

Fig. 1. The phase shift (*solid line*) and the negative of the imaginary part of the reactance matrix (*dashed line*) as a function of the real part of the energy in the vicinity of the $v=11$, $J=13$ resonance on the WB potential. For the reactance matrix, the imaginary part of the energy is fixed at -0.01 cm^{-1} while for the phase shift, the energy is real. The stepsize used for both calculations is $h=0.01a_0$

3.4. The large r potential

The potentials for atom-atom scattering behave at large r as r^{-6} (we ignore long range relativistic retardation effects). In our calculations, however, when we stop the integration of Eq. (1) at r_{asy} to perform an asymptotic analysis, we assume the potential is zero for r larger than r_{asy}. Usually at real energies it is a fairly easy matter to converge the calculations with respect to increasing r_{asy}, and then the difference between an infinitely ranged r^{-6} potential and a finite ranged one is not important. The situation seems to be different when complex energies are involved. Empirically we observed that as r_{asy} was increased, the location of the poles of the scattering matrix moved. The general pattern was a clockwise spiral which seemed to converge to a circle, rather than to a point. An example of this is shown in Fig. 2 for the broad $v=14$, $J=6$ resonance. These features were present in all of the resonances for which we carefully checked convergence with respect to r_{asy}, and the radius of the circle appears to be approximately proportional to the imaginary part of k_1. Thus resonances with $\mathscr{E}_\alpha \gg \Gamma_\alpha$ will have small radii, and so the resonance parameters will converge to a satisfactory number of digits as r_{asy} is increased. Note that r_{asy} cannot be made arbitrarily large because one of the matching functions grows as $\exp[|\mathrm{Im}\,(k_1)|r]$. If a matching function becomes too large, it will not be possible to accurately calculate the scattering matrix since the growth of the matching function in Eq. (44) is counterbalanced by the cancellation of two terms, and the finite precision available on the computer limits the amount of cancellation which can occur.

The probable cause of the circles as a function of r_{asy} can be seen by more carefully considering the analyticity of the scattering matrix. For simplicity, we

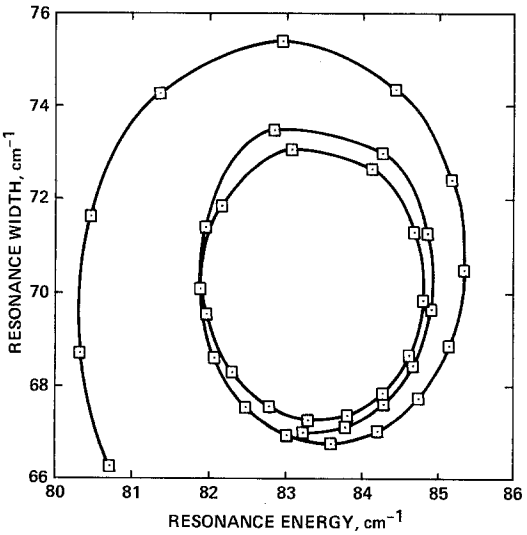

Fig. 2. The resonance energy and width as a function of r_{asy} for the $v=14$, $J=6$ resonance on the WB potential. The symbols mark an evenly spaced grid of r_{asy} going from 10 to $20a_0$. The stepsize used for all points is $h=0.01a_0$

consider only the one channel case in this discussion, and so channel subscripts will be eliminated. It is most convenient to formulate the calculation of the scattering matrix in terms of the Jost functions $f_l(k)$ which are defined by [3]

$$f_l(k)=1+k^{-1}\hbar^{-3}2i\mu\int_0^\infty dr h_l^{(1)}(kr)V(r)\phi_{l,k}(r), \tag{49}$$

where $\phi_{l,k}$ is the solution of Eq. (1) with boundary condition $\phi_{l,k}(r)\sim j_l(kr)$ as $r\sim 0$. The scattering matrix is then given by

$$S(k)=f_l(-k)/f_l(k). \tag{50}$$

As the energy becomes complex, so that k has a nonzero imaginary part, the product $h_l^{(1)}\phi_{l,k}$ will grow as exp [2 Im (k)]. The Jost functions may then become undefined because the integral in Eq. (49) may not converge at large r. This is not a problem if the potential goes to zero fast enough as r increases. In particular, any potential with a finite range will cause the integral in Eq. (49) to be only over a finite range and consequently to not diverge. It is pointed out by Newton [26] that this means that the results for a potential truncated at r_{asy} will not converge to the results for the untruncated potential as r_{asy} is increased. It is this affect which seems to cause the circles as r_{asy} is increased.

This poses the question of what are the accurate resonance parameters, that is the ones obtained when the potential is not truncated. However, we must keep in mind that due to the uncertainty principle, the finite nonzero lifetime of the resonance states places a limit on the precision of the resonance parameters which have any meaning. Another aspect of the problem is that under experimental

conditions, there is a limit as to how far apart the atoms can become until their interaction is screened away by the presence of other objects. Thus even if parameters were obtained for the untruncated potential, these would not be directly applicable to any experimental situation.

3.5. The extrapolation of the results

As discussed previously in Sect. 3.2 we solve the scattering problem exactly for a potential which differs from the exact one by being piecewise constant with stepsize h (in the present calculations, we take all sectors to have equal widths). The resonance parameters will depend on the stepsize h and what we desire is the values obtained in the limit as h goes to zero. This can be accomplished in two ways. First of all, we can perform a calculation with h small enough so that the results obtained are acceptably close to the zero stepsize values. Alternatively, we can perform calculations at a sequence of larger stepsizes, and extrapolate to zero stepsize.

We will consider two extrapolation procedures [19]. The first is the Richardson extrapolation whereby the results are fitted to a polynomial in powers of h^2. The second is rational function extrapolation whereby the results are fitted to the ratio of two polynomials in powers of h^2. Table 1 shows the results of these procedures using the stepsize pattern $(h, h/2, h/3, h/4, h/6, h/8, h/12, \ldots)$. Both extrapolation procedures yield results which converge much faster than when not using extrapolation. In our production calculations, we perform calculations at the first four stepsizes shown in this table and extrapolate the results to zero stepsize. In almost all cases, the two extrapolation methods agree after four stepsizes to more digits then we quote in the tables, and when they do not agree very well, we perform calculations at additional stepsizes until they do agree.

Table 1. Resonance energy and width as a function of stepsize for $J = 13$ resonance. The WB potential is used with μ atomic. The stepsize is h_0/n, $h_0 = 0.1a_0$. The energy units are cm^{-1} and the width is multiplied by 10^3

n	No extrapolation		Richardson extrapolation		Rat. function extrapolation	
	$\mathscr{E}_\alpha$	Γ_α	$\mathscr{E}_\alpha$	Γ_α	$\mathscr{E}_\alpha$	Γ_α
1	204.085	6.624	...	...	...	...
2	200.648	5.343	199.502	4.916	199.528	5.019
3	199.955	5.114	199.387	4.932	199.386	4.932
4	199.708	5.034	199.388	4.933	199.388	4.933
6	199.530	4.978	199.388	4.933	199.388	4.933
8	199.468	4.958	199.388	4.933	199.388	4.933
12	199.423	4.944	199.388	4.933	199.388	4.933
16	199.408	4.939	199.388	4.933	199.388	4.933
24	199.397	4.936	199.388	4.933	199.388	4.933
32	199.393	4.935	199.388	4.933	199.388	4.933
48	199.390	4.934	199.388	4.933	199.388	4.933

The behavior of the poles as a function of stepsize shown in Table 1 is typical, with the large stepsize calculations giving resonance energies which differ by several cm^{-1} from the accurate values. Thus if the width is less than about 0.1 cm^{-1}, an initial guess which is the accurate value, or even the value obtained at the last stepsize, will not be sufficiently close to the pole energy for the current stepsize for the Newton-Raphson procedure to converge. This is why it is necessary to have a good method of approximately locating the poles such as that given in Sect. 3.3.

The Richardson extrapolation procedure used here is similar to that used by Anderson [27] except that there he extrapolated state-to-state probabilities and used polynomials in h^2 which excluded the h^2 term. The Magnus propagator used by both of us has a leading error term proportional to h^2, however, for the problem of [27], for some reason the coefficient of the h^2 term is zero thus giving a leading error term proportional to h^4. For the present application we empirically determined that faster convergence was obtained when all powers of h^2 are included.

4. Potentials

We consider several different potential functions and these are now discussed. Initial tests were carried out on the WB potential, which is an analytic representation by Waech and Bernstein [11] to the 1965 Kołos and Wolniewicz, Born-Oppenheimer potential [28]. This potential was also used in the calculations of [12].

We next consider a slightly more accurate Born-Oppenheimer potential, and call it BO. This is a fit to the more recent data of [16]. For r between the limits of their tabulated data, the potential is interpolated by a quintic polynomial with coefficients determined by exactly fitting [29] r^2V and dr^2V/dr at the nearest three points. The potential is extrapolated to larger r using $-C_6/r^6-C_8/r^8$ and to smaller r with an exponential with the coefficients determined by continuity of the potential and its derivative.

The remaining potentials include corrections to the Born-Oppenheimer potential. For all but the nonadiabatic corrections, we approximately follow the procedure of [15]. The next potential is obtained by adding a relativistic correction to BO; the result is called Rel. The relativistic correction is taken from [30]. For r less than $0.6a_0$, the correction is represented as an exponential with parameters determined from the value of the function and a forward difference estimate of its derivative at $0.6a_0$. For r greater than $3.6a_0$, exponential decay to the asymptotic value is used with an exponential parameter of $1a_0^{-1}$ and the remaining parameters determined from the $3.6a_0$ and ∞ data. Intermediate distances are interpolated by a cubic spline which is forced to have continuous functions and derivatives when the boundaries at 0.6 and $3.6a_0$ are crossed. To make the spline smooth, the data points at 1.401 and $1.4011a_0$ where not included in the fit.

To the Rel potential, we added a correction for radiative effects to produce a

potential called Rad. This correction was determined as in [15] and fit by the same procedure described above for the relativistic correction.

The final correction that can be represented as a state independent potential correction is the adiabatic nuclear motion correction which is added to the Rel potential to give the one called Ad. The data for this correction is taken from [15] and [30] with the results from [30] adjusted for a change in mass by multiplying by the factor $1836.12/2\times 918.0764$. Some points from [30] were also scaled and shifted as described in [15]. For r less than $0.4a_0$, the data is extrapolated using an exponential with parameters determined from the value of the function and a forward difference estimate of its derivative at $0.4a_0$. For r greater than $8a_0$, exponential decay to the asymptotic value is used with the parameters determined by fitting the data at 7 and $8a_0$. At intermediate distances, cubic spline interpolation is used with the spline required to have continuous functions and derivatives when the boundaries at 0.4 and $8a_0$ are crossed.

The final correction is for nonadiabatic effects and cannot be represented as a simple addition to the potential in Eq. (1). It is not an easy task to include these effects exactly, however, it has been shown that for bound states approximate corrections can work quite well [31]. Thus we will base our estimates of non-adiabatic effects on solutions of an effective Schrödinger equation which we write following [31] as

$$d^2f(r)/dr^2=[1+\alpha(r)]\{[1-\alpha'(r)]J(J+1)/r^2-k^2+2\mu\hbar^{-2}V(r)]\}f(r), \qquad (51)$$

where the channel subscripts for the present one channel application have been dropped and α and α' are correction terms approximated by [31]

$$\alpha(r)=\kappa F(r)/3 \qquad (52)$$

and

$$\alpha'(r)=\kappa' 2F(r)/3, \qquad (53)$$

where κ and κ' are empirical parameters and $F(r)$ is the function given as column 8 of Table III of [30]. In our calculations $F(r)$ is represented in three regions similarly as with the other corrections. For r less than $0.6a_0$, we use $A[1-\exp(-Br)]$, with A and B determined from the first two data points. For r greater than $3.1a_0$, exponential decay to the asymptote is used with parameters determined from the data at 3.0 and $3.1a_0$. Intermediate distances are interpolated using a cubic spline with continuous functions and derivatives across the boundaries at 0.6 and $3.1a_0$. The tabulated data points for r in the range $3.2-3.7a_0$ are not included in the fit because when they were included, the spline fit was not very smooth. In the bound state calculations of [31], $\alpha'(r)$ was neglected and κ was adjusted to obtain the best agreement with experimental vib-rotational energies. In the present case, we use a slightly different procedure. The parameter κ is determined by optimizing the agreement between the bound state energy levels for $J=0$ calculated from Eq. (51) and those calculated from the Ad potential corrected by the v, J dependent factors of [15]. The energy levels are calculated using the FDBV method using a reduced mass equal to 918.07575 a.u. As discussed

in [14], there may be some errors in the factors tabulated in [15] for high v, so to avoid this possible problem, we only consider energy levels with $v \leq 11$ in the optimization process. This yields $\kappa = 3.46 \times 10^{-5}$ as compared to the value $\kappa = 3.55 \times 10^{-5}$ obtained by Bishop and Shih [31]. This value of κ gives energy levels which have an rms error of only 0.056 cm^{-1} and a maximum error of 0.131 cm^{-1} when compared to the accurate values. Once κ is fixed, we optimize κ' by a similar procedure by minimizing the difference between the accurate energies and the ones obtained from Eq. (51) for all states with $v \leq 11$ and $J \leq 31$. This produces $\kappa' = 6.50 \times 10^{-6}$ and gives an rms error of 0.61 cm^{-1} and a maximum error of 2.2 cm^{-1}, which is not as good a fit as for the $J = 0$ case, but still much better than no nonadiabatic corrections at all. When Eq. (51) is used with these values of κ and κ', the potential will be called Nonad. For this potential, it is necessary to multiply Eqs. (40) and (42) by the factor $1 + \alpha(r)$. In principle for this potential, l in Eqs. (5)-(6) should be replaced by $\sqrt{A(l+1/2)^2 + (1-A)/4} - 1/2$, where A is the product of the asymptotic values of α and α', however, since as $r \sim \infty$, l only enters as a phase in the matching functions and A will not be significantly different from unity, we will ignore this replacement.

The calculations including nonadiabatic effects give a dissociation energy of the ground state of H_2 as 36,118.093 (accurate) and 36,118.071 cm^{-1} [Eq. (51)] which are just within the experimental error bars (36,118.60 ± 0.5 cm^{-1} [34]). Our accurate calculation also agrees well with the results of [16] (we differ by 0.005 cm^{-1}) and the results of [14] (we differ by 0.019 cm^{-1}). The only difference between our accurate calculation and that of [16] is the fitting procedures used for the various potentials and the method used for solving the Schrödinger equation (we use the FDBV method), while an additional difference with the procedure of [14] is a slightly different value of the hydrogen mass is used (we use 1836.1515 a.u. = 1.007276644u vs. 1.007276470u).

5. Results and discussion

Table 2 shows resonance parameters calculated using the present new method for the several different potentials and compares them to the results of [12]. The particular subset of resonances shown in this table is the same as [12]. In Tables 3 and 4, we show the results for additional resonances.

Column 4 of Table 2 should differ from the results of [12] only in the method used to calculate the resonance parameters. The particular results quoted from [12] and given in column 3, are the ones which correspond to those calculated from methods which mimic scattering experiments. The agreement between the two columns is quite good for the resonance energies, with differences typically a fraction of a wave number. There are larger differences in the resonance widths, especially for broader resonances, but on the whole the agreement between the two methods is quite good.

The next column in Table 2 (column five), differs only from column four in the value of the reduced mass used. Except for the fourth column in Table 2, all our calculations use, as the reduced mass of H_2, the nuclear reduced mass

Table 2. Resonance parameters for selected resonances for various potential approximations. All energies are in cm^{-1}. The first row is the resonance energy, the second is the resonance width and the third is the partial width

v	J	[12]	WB[a]	WB	BO	Rel	Rad	Ad	Nonad
0	38	7510.0[b]	7510.93	7520.98	7517.55	7518.15	7518.10	7506.67	7502.49
		80.0[c]	87.10	88.89	89.44	89.58	89.57	86.46	85.82
		...	101.18	103.58	104.34	104.52	104.52	100.31	99.47
0	37	6513.3	6515.79	6526.61	6523.47	6524.15	6524.10	6510.86	6506.51
		5.84	6.021	6.261	6.335	6.353	6.352	5.948	5.863
		...	6.069	6.313	6.389	6.407	6.406	5.995	5.909
1	35	5549.8	5551.18	5560.75	5557.34	5557.94	5557.90	5546.79	5542.76
		14.1	14.51	15.06	15.22	15.26	15.26	14.40	14.19
		...	14.80	15.38	15.55	15.59	15.59	14.69	14.47
2	33	4688.4	4689.09	4697.60	4694.02	4694.55	4694.52	4685.06	4681.33
		20.4	20.93	21.71	21.95	22.01	22.01	20.86	20.53
		...	21.57	22.39	22.65	22.71	22.71	21.49	21.14
3	31	3925.0	3925.23	3932.81	3929.07	3929.55	3929.52	3921.39	3917.91
		23.6	24.21	25.10	25.38	25.44	25.44	24.19	23.78
		...	25.07	26.03	26.33	26.40	26.40	25.05	24.61
4	29	3254.7	3254.79	3261.54	3257.63	3258.05	3258.03	3251.01	3247.77
		24.7	25.31	26.26	26.52	26.58	26.58	25.32	24.85
		...	26.26	27.29	27.57	27.64	27.64	26.27	25.77
5	27	2673.0	2673.01	2678.97	2674.87	2675.25	2675.23	2669.19	2666.18
		25.1	25.72	26.71	26.97	27.04	27.04	25.80	25.28
		...	26.71	27.78	28.07	28.14	28.14	26.80	26.24
6	25	2175.0	2174.96	2180.16	2175.88	2176.21	2176.20	2171.05	2168.29
		26.5	27.09	28.13	28.36	28.43	28.42	27.18	26.61
		...	28.20	29.33	29.59	29.66	29.66	28.31	27.68
7	23	1755.3	1755.13	1759.59	1755.14	1755.43	1755.42	1751.13	1748.64
		30.4	31.12	32.26	32.46	32.53	32.53	31.22	30.54
		...	32.59	33.84	34.08	34.17	34.17	32.72	31.98
8	21	1407.0	1406.79	1410.48	1405.91	1406.16	1406.15	1402.69	1400.51
		39.4	40.44	41.79	41.93	42.02	42.02	40.52	39.68
		...	42.89	44.40	44.61	44.71	44.71	43.02	42.08
9	19	1121.6	1121.28	1124.20	1119.52	1119.72	1119.71	1117.05	1115.24
		57.9	59.61	61.29	61.40	61.51	61.51	59.71	58.59
		...	64.36	66.29	66.58	66.71	66.71	64.63	63.38
9	18	725.9	725.87	730.05	725.75	726.04	726.03	721.83	719.11
		0.52	0.5244	0.5718	0.5559	0.5592	0.5592	0.5092	0.4794
		...	0.5246	0.5721	0.5562	0.5595	0.5595	0.5095	0.4796
10	16	586.0	585.91	589.11	584.70	584.93	584.93	581.81	579.61
		2.92	2.919	3.125	3.024	3.038	3.038	2.826	2.686
		...	2.928	3.136	3.034	3.049	3.049	2.836	2.695
11	14	480.1	479.97	482.11	477.63	477.78	477.78	475.78	474.24
		17.9	17.93	18.70	18.14	18.19	18.19	17.43	16.87
		...	18.27	19.06	18.50	18.56	18.56	17.77	17.19
11	13	199.4	199.39	202.59	198.22	198.45	198.45	195.25	192.84
		0.0053	0.004926	0.005966	0.004839	0.004908	0.004908	0.004014	0.003439
		...	0.004926	0.005966	0.004839	0.004907	0.004908	0.004014	0.003439
12	12	385.0	384.91[d]	386.10	381.42	381.51	381.51	380.47	379.60
		74.5	71.60	73.19	70.91	71.02	71.03	69.49	68.28
		...	69.00	70.36	68.65	68.75	68.75	67.42	66.48
12	11	215.5	215.47	217.41	213.21	213.36	213.36	211.48	209.94
		2.63	2.615	2.829	2.517	2.532	2.532	2.335	2.182

Table 2—continued

v	J	[12]	WB[a]	WB	BO	Rel	Rad	Ad	Nonad
		...	2.621	2.836	2.522	2.537	2.538	2.340	2.187
13	9	195.0	194.69	195.44	191.88	191.95	191.95	191.26	190.56
		56.6	51.47	52.69	49.32	49.41	49.41	48.28	47.33
		...	45.11	45.92	43.61	43.67	43.68	42.89	42.52
13	8	89.9	89.91	91.23	87.45	87.55	87.56	86.26	85.12
		1.90	1.871	2.059	1.630	1.643	1.643	1.485	1.353
		...	1.871	2.060	1.631	1.644	1.644	1.485	1.354
14	6	81.9	84.26[d]	84.51	82.41	82.43	82.43	82.29	82.11
		115.	72.96	74.25	68.73	68.84	68.84	67.60	65.87
		...	42.97	43.16	42.67	42.75	42.75	41.81	38.83
14	5	45.7	45.79	46.18	44.17	44.21	44.21	43.82	43.46
		29.5	17.65	18.28	15.74	15.79	15.79	15.22	14.69
		...	14.50	14.89	13.26	13.29	13.29	12.90	12.53
14	4[e]	3.76	3.756	4.516	1.566	1.632	1.633	0.8420	0.088
		0.0060	0.00586	0.0129	1.32(−4)[f]	1.58(−4)	1.59(−4)	8.38(−6)	<1(−9)
		...	0.00586	0.0129	1.32(−4)	1.58(−4)	1.59(−4)	8.38(−6)	<1(−9)

[a] This column uses μ_{atomic} while all others use μ_{nuclear}

[b] The first row is the resonance energy. We quote the column labeled $r_d(\max)$ from [12]

[c] The second row is the resonance width. We quote the column labeled $2/[\pi c \tau_d(\max)]$ from [12]

[d] This resonance has Im k large enough so that the results do not converge with respect to increasing r_{asy}. These results use $r_{asy} = 20a_0$

[e] We use extrapolation based on 6 stepsizes for this resonance

[f] $1.32(-4) = 1.32 \times 10^{-4}$

(918.07575 a.u. [16]), while the fourth column uses a value of the atomic reduced mass (918.575728 a.u.) which was apparently used by [12]. The nuclear reduced mass is the one which is consistent with the Born-Oppenheimer approximation and corrections to it. The effect of changing the reduced mass is fairly large with the resonance energies increasing by up to about 11 cm^{-1} when the nuclear reduced mass is used. The larger resonance widths are increased by about 1 cm^{-1} and the smaller widths are increased by fairly large factors.

The next columns show the effect of using different potentials. Changing from the WB approximate fit to Born-Oppenheimer data to the more accurate BO potential causes a decrease in the resonance energies and in fact many of the resonance energies from the BO potential agree fairly well with the results from the WB potential using the atomic reduced mass. The resonance widths are usually increased by this change, but not always. Larger widths change by several tenths of wave numbers while the narrow widths decrease, in some cases dramatically. Adding relativity increases the resonance energies slightly, typically by a few tenths of a wave number. The change in the resonance widths is similar, although usually smaller. For most resonances, adding the radiative correction causes a negligible change in the resonance parameters. Including the adiabatic nuclear motion correction lowers the resonance energies and decreases the resonance widths by a fairly large amount—this correction causes the largest change

Table 3. Resonance parameters for additional resonances with narrow widths on the Ad and Nonad potentials. Energies are in cm^{-1}. The first row is the resonance energy and the second is the resonance width[a]

v	J	Ad		Nonad	Experiment[c]
		FDBV/WKB[b]	Accurate	Accurate	
0	36	5414.3	5414.32	5409.82	
		0.0547	0.06077	0.05943	
0	35	4243.24	4243.24	4238.71	
		7.46(−5)[d]	8.284(−5)	8.025(−5)	
0	34	3016.77		3012.26[e]	
		5.47(−9)		5.22(−9)	
1	34	4535	4534.92	4530.59	
		0.131	0.1375	0.1340	
0	33	1744.44		1739.97[e]	
		8.84(−16)		8.13(−16)	
1	33	3433.34	3433.34	3428.89	
		1.04(−4)	1.091(−4)	1.050(−4)	
0	32	432.68		428.28[e]	
		6.04(−34)		4.31(−34)	
1	32	2271.16		2266.68[e]	
		1.78(−9)		1.68(−9)	
2	32	3750.6	3750.57	3746.40	
		0.166	0.1707	0.1658	
1	31	1061.27		1056.79[e]	
		1.49(−18)		1.30(−18)	
2	31	2716.74	2716.74	2712.38	
		6.55(−5)	6.780(−5)	6.476(−5)	
2	30	1619.48		1615.03[e]	
		1.38(−10)		1.28(−10)	
2	29	474.14		469.65[e]	
		8.18(−25)		6.15(−25)	
3	30	3059.40	3059.39	3055.36	
		0.155	0.1578	0.1526	
3	29	2092.99	2092.99	2088.70	2088.59
		2.54(−5)	2.603(−5)	2.462(−5)	
3	28	1062.40		1057.98[e]	
		2.08(−12)		1.85(−12)	
4	28	2459.3	2459.34	2455.46	
		0.124	0.1258	0.1211	
4	27	1561.58	1561.58	1557.38	1556.93
		6.75(−6)	6.876(−6)	6.413(−6)	
4	26	600.44		596.06[e]	595.50
		1.92(−15)		1.58(−15)	
5	26	1948.3	1948.26	1944.53	1943.99
		0.0968	0.09753	0.09329	
5	25	1121.73	1121.73	1117.63	1117.20
		1.33(−6)	1.343(−6)	1.230(−6)	
5	24	233.77		229.44[e]	228.57
		1.12(−21)		7.06(−22)	
6	24	1523.5	1523.54	1519.98	1519.45
		0.0833	0.08361	0.07946	
6	23	772.07	772.07	768.08	767.81
		2.15(−7)	2.160(−7)	1.925(−7)	

Table 3—continued

v	J	Ad		Nonad	Experiment[c]
		FDBV/WKB[b]	Accurate	Accurate	
7	22	1181.7	1181.63	1178.28	1177.76
		0.0933	0.09286	0.08773	
7	21	510.08		506.26[e]	506.33
		3.69(−8)		3.16(−8)	
8	20	917.1	917.19	914.11	914.03
		0.163	0.1610	0.1514	
8	19	331.40		327.78[e]	328.15
		1.29(−8)		1.05(−8)	
9	18	721.9	721.83	719.11	718.96
		0.526	0.5092	0.4794	
9	17	228.65		225.31[e]	225.10
		3.55(−8)		2.76(−8)	
10	15	189.78	189.78	186.83	186.51
		3.24(−6)	3.21(−6)	2.51(−6)	
11	13	195.25	195.25	192.84	192.54
		4.17(−3)	4.014(−3)	3.439(−3)	

[a] All resonances in this table have partial widths which differ by less than 0.1% from the resonance width

[b] The resonance energy is calculated using the FDBV method and the width is found using the semiclassical formula evaluated at the FDBV energy

[c] The excitation energies of [35] have the theoretical $D_0 = 36118.07\ \text{cm}^{-1}$ subtracted from them

[d] $7.46(-5) = 7.46 \times 10^{-5}$

[e] This resonance is too narrow to use the accurate method so the FDBV/WKB method is used instead

of any of the other potential variations. Some resonance energies change by as much as $13\ \text{cm}^{-1}$ and there are widths which change several wave numbers. Approximately including nonadiabatic effects causes a further decrease of the resonance parameters, with changes on the order of wave numbers for the resonance energies and fractions of wave numbers for the widths.

The partial widths are also shown in Table 2. These parameters change with various potential modifications in a similar manner as the resonance widths. As mentioned in Sect. 2, for resonances which satisfy the INR hypothesis, the partial width should equal the resonance width. Of all the resonances with parameters given in Table 2, this equality only holds for the narrowest resonances. For broader resonances, it is most likely that the partial width will be greater than the resonance width, but this is not always so.

An interesting resonance to single out from Table 2 is the one with $v = 14$, $J = 4$. This state is almost bound and its resonance parameters are very sensitive to changes in the potential with the resonance energy ranging from 4.516 to $0.088\ \text{cm}^{-1}$ and the width ranging from 0.0129 to $< 1 \times 10^{-9}\ \text{cm}^{-1}$. Experimentally, this state appears to be bound, however, its binding energy of $0.48\ \text{cm}^{-1}$ (from the excitation energy from [35] and the dissociation energy of [34]) is less than the error bars of the dissociation energy ($0.5\ \text{cm}^{-1}$). There has been some debate

Table 4. Resonance parameters for additional resonances with wide widths on the Ad and Nonad potentials. Energies are in cm^{-1}. The first row is the resonance energy, the second is the resonance width and the third is the partial width

v	J	Ad	Nonad
1	36	6443	6439
		166	164
		216	215
2	34	5497	5493
		218	217
		305	302
3	32	4657	4653
		247	245
		355	354
4	30	3914	3911
		259	258
		374	375
5	28	3263	3260
		264	263
		378	380[a]
6	26	2695	2693
		268	266
		375	370[a]
10	17	883	882
		96.3	94.8
		105	103
11	15	687	687
		159	158
		160	160

[a] This parameter has an uncertainty of about $10\ cm^{-1}$

about whether or not it should be included when calculating three body recombination rates [2, 32, 33]. In practice, however, it is probably not important whether or not this state is really bound when the kinetics are carefully taken into account for it is unlikely that there is a difference between an infinite lifetime and a lifetime greater than 0.005 s.

In Table 3 the remaining narrow resonances (widths less than $1\ cm^{-1}$) are given along with experimental resonance energies when they are available [35]. The widths range from 0.17 to $6\times10^{-34}\ cm^{-1}$. The agreement with experimental energies is very good for the Nonad potential (the rms error is $0.42\ cm^{-1}$), in fact it is slightly better than can be expected based upon the errors found in the calibration process (rms error $0.61\ cm^{-1}$). This contrasts with an rms error of $3.99\ cm^{-1}$ when nonadiabatic effects are ignored and the Ad potential is used. Also given in Table 3 are the results of the FDBV method used to determine the resonance energies and the WKB [Eq. (46)] method to determine the widths.

The FDBV method gives energies for these narrow resonances which agree very well with the accurate ones. The widths from the WKB method are not as accurate, with about 10% error for the resonances with $v = 0$. As v increases, the widths become more accurate, and for large v, agree within about 1% with the accurate values.

Table 4 contains the results for resonances with larger widths. These show similar trends as the broader resonances in Table 2. There appear to be no other resonances not included in Tables 2 to 4 which have widths smaller than about 200 cm^{-1} on the Ad potential, however, there are many with larger widths. In fact, potentials such as the ones used here have an infinite number of resonances [3]. However, most of these resonances are not of physical interest, since they will have increasing widths and the distinction between resonant and background scattering will be miniscule.

6. Conclusions

We have developed a new method to calculate resonance parameters and applied it to the hydrogen molecule. The new method works very well and should be applicable to a wide variety of problems. An important ingredient of the method is the accurate calculation of derivatives of the scattering matrix with respect to the energy. It is expected that this quantity can be used to advantage in other situations besides the one described here. One possible extension might be to calculate derivatives of the scattering matrix with respect to potential parameters [36]. However, this would introduce new complications and hence require some modifications of the present procedure.

A subset of the H_2 resonances are considered on several different potentials which differ in the inclusion of corrections to the Born-Oppenheimer potential. The correction which has the largest effect is the adiabatic nuclear motion correction. Nonadiabatic effects are also included in an approximate manner, and they are also significant. It is also important to use the nuclear reduced mass rather than the atomic reduced mass in the calculations so as to be consistent with the Born-Oppenheimer approximation and its corrections.

References

1. Simons J (1984). In: Truhlar DG (ed) Resonances. American Chemical Society, Washington, pp 3-16
2. Roberts RE, Bernstein RB, Curtiss CF (1969) J Chem Phys 50:5163-5176
3. Taylor JR (1983) Scattering theory. Krieger, Malabar, Fla
4. Ashton CJ, Child MS, Hutson JM (1983) J Chem Phys 78:4025-4039
5. Hayes EF, Walker RB (1984). In: Truhlar DG (ed) Resonances. American Chemical Society, Washington, pp 493-513
6. Bartschat K, Burke PG (1986) Computer Phys Commun 41:75-84
7. Schwenke DW, Truhlar DG (1987) J Chem Phys 87:1095-1106
8. LeRoy RJ, Liu W-K (1978) J Chem Phys 69:3622-3631
9. Basilevsky MV, Ryaboy VM (1981) Int J Quantum Chem 19:611-635; (1984) Chem Phys 86:67-83; (1987) J Comp Chem 8:683-699
10. Watson DK (1984) Phys Rev A 29:558-561; (1986) 34:1016-1025; (1986) J Phys B 19:293-299

11. Waech TG, Bernstein RB (1967) J Chem Phys 46:4905–4911
12. LeRoy RJ, Bernstein RB (1971) J Chem Phys 54:5114–5126
13. LeRoy RJ (1971) J Chem Phys 54:5433–5434
14. Schwartz C, LeRoy RJ (1987) J Mol Spect 121:420–439
15. Wolniewicz L (1983) J Chem Phys 78:6173–6181
16. Kołos W, Szalewicz K, Monkhorst HJ (1986) J Chem Phys 84:3278–3283
17. Weidenmüller HA (1964) Ann Phys 28:60–115; (1964) 29:378–382
18. Hazi A (1979) Phys Rev A 19:920–922
19. Press WH, Flannery BP, Teukolsky SA, Vetterlin WT (1986) Numerical recipes. Cambridge University Press, Cambridge
20. Light JC, Walker RB (1976) J Chem Phys 65:4272–4282; Stechel EB, Walker RB, Light JC (1978) J Chem Phys 69:3518–3531
21. Dickinson AS (1974) Mol Phys 28:1085–1089
22. Rush DG (1968) Trans Faraday Soc 64:2013–2016
23. Truhlar DG (1972) Chem Phys Let 15:483–485
24. Truhlar DG (1974) Chem Phys Let 26:377–380
25. Ford KW, Hill DL, Wakano M, Wheeler JA (1959) Ann Phys 7:239–258
26. Newton RG (1982) Scattering theory of waves and particles, 2nd edn. Springer, New York Heidelberg Berlin
27. Anderson RW (1982) J Chem Phys 77:4431–4440
28. Kołos W, Wolniewicz L (1965) J Chem Phys 43:2429–2441
29. LeRoy RJ, Bernstein RB (1968) J Chem Phys 49:4312–4321
30. Kołos W, Wolniewicz L (1964) J Chem Phys 41:3663–3673
31. Bishop DM, Shih S-K (1986) J Chem Phys 64:162–169
32. Menzinger M (1971) Chem Phys Let 10:507–509
33. Walkauskas LP, Kaufman F (1976) J Chem Phys 64:3885–3886
34. Stwalley WC (1970) Chem Phys Let 6:241–244
35. Dabrowski I (1984) Can J Phys 62:1639–1664
36. Guzman R, Rabitz H (1987) J Chem Phys 86:1387–1394